

ADSORPTION OF DIAZO DYE DIRECT RED-28 AND TETRA-AZO DYE DIRECT BLACK-22 USING CALCINED KAOLIN IN AQUEOUS SOLUTIONS

Serap Findik*

Hitit University, Engineering Faculty, Chemical Engineering Department, Kuzey Kampusu, Çorum, Türkiye

(Received July 22, 2022; Revised December 22, 2022; Accepted December 28, 2022)

ABSTRACT. In this study, the removal of diazo and tetra-azo dyes using calcined kaolin were compared. Direct red-28 (DR-28) and Direct black-22 (DB-22) was chosen as diazo and tetra-azo dyes, respectively. The kaolin obtained from Türkiye and calcined at 200 °C was found to be the most efficient adsorbent. Natural and calcined kaolins were characterized using SEM-EDS, FTIR, TGA, and XRD. The parameters such as, calcination temperature of the kaolin, adsorbent amount, temperature, initial pH, contact time, and initial concentration were studied. It was found that the removal rate of DR-28 was higher than that of DB-22 at the studied conditions. The removal of DR-28 and DB-22 were found to be 90.1% and 46.2% under the following conditions: adsorbent amount: 1.2 g/200 mL, initial concentration: 20 mg/L, original pH, temperature: 20 °C and contact time 120 min. The adsorption of the dyes was fitted to Langmuir isotherm model. The maximum adsorption capacity of calcined kaolin at 200 °C was determined as 5.39 and 3.5 mg/g for DR-28 and DB-22, respectively. The adsorption of DR-28 and DB-22 followed a pseudo-second order model. The thermodynamic study showed that the adsorption of DB-22 onto calcined kaolin was endothermic while that of DR-28 was exothermic.

KEY WORDS: Adsorption, Diazo dye, Tetra-azo dye, Kaolin

INTRODUCTION

Textile industries generate a large amount of wastewater with synthetic dyestuffs, which causes environmental pollution. Small quantities of dye (< 1 mg /L) can color a large body of water. Due to their toxic, carcinogenic, and mutagenic properties, dyes used in textile industry are dangerous chemicals. Dyes have a negative effect on the living substances, aquatic animal life, and water quality. Coloring agent in the wastewater prevents sunlight penetration and photosynthesis, and alters gas solubility. Pollutants in wastewater reach people through the food chain [1-4]. For these reasons, it is environmentally important to remove dyes from wastewater.

Dyes are colored organic compounds based on three essential groups in their molecules: chromophore, auxochrome and matrix. The chromophore consists of groups of atoms such as nitro ($-\text{NO}_2$), azo ($-\text{N}=\text{N}-$), nitroso ($-\text{N}=\text{O}$), thiocarbonyl ($-\text{C}=\text{S}$), carbonyl ($-\text{C}=\text{O}$) and alkenes ($-\text{C}=\text{C}-$). The atom group is attached to the chromophore called auxochrome. The purpose of using auxochrome groups is to fix the dyes and modify their color. The auxochrome groups may be acidic such as OH, SO_3 and COOH or basic such as NHR, NH_2 and NR_2 . The third part of the dye, called the matrix (benzene, perylene and anthracene rings), contains the remaining atoms of the molecule [5-7]. Dyes can be classified according to their application area: acid, basic, reactive, direct, disperse, and vat dyes. Dispersed and vat dyes are insoluble in water while others are water soluble. Water soluble dyes are mostly used in nylon, wool, cotton, leather, and paper dyeing [5, 7].

Azo dyes contain at least one azo group. Depending on the number of azo groups they contain, they are called monoazo, disazo, triazo, or poly-azo dye. Poly-azo dyes are complex and their azo groups are repeated three or more times in the same molecule. About 70% of the dyes used in textile production are azo dyes [8].

*Corresponding author. E-mail: serapfindik@hitit.edu.tr

This work is licensed under the Creative Commons Attribution 4.0 International License

Direct red-28 (DR-28) ($C_{32}H_{22}N_6Na_2S_2O_6$) is an anionic dye that causes cancer in humans. The other known name of the DR-28 is Congo red. It contains two azo groups. DR-28 is obtained by the reaction of tetrazotized benzidine with two molecules of naphthionic acid. It can stay in the environment for a long time [9-12]. DR-28 is used in pharmaceutical, paper, plastics, printing and textile industries [12]. Direct black-22 (DB-22) ($C_{44}H_{32}N_{13}Na_3O_{11}S_3$) is one of the toxic and carcinogenic anionic azo dyes used in dyeing cellulosic fibers like cotton, wool, viscose, rayon and paper. It contains tetra-azo groups. It is difficult to remove of DB-22 due to its stability and recalcitrant property [8, 13].

Several treatment methods are used to remove dye solutions such as adsorption [11], photocatalysis [14, 15], coagulation [16], Fenton [17], ozonation [18] and sonication [19] etc. These methods have some limitations and disadvantages such as low efficiency, high energy consumption, high chemical consumption, sludge disposal [13].

Among these, adsorption process attracts more attention compared to other conventional treatment methods due to its low initial cost, high efficiency, easy operation, and insensitivity to pollutants and toxic compounds. Adsorption process becomes more economic with low-cost adsorbents [1, 11].

Kaolin is one of the low-cost, eco-friendly, and efficient adsorbents with a chemical structure of $Al_2O_3 \cdot 2SiO_2 \cdot 2H_2O$. Highly abundant in nature, it is a white and soft plastic clay with high thermal and mechanical stability. Kaolin structure contains hydrated aluminum silicate, kaolinite, quartz, and mica. The silicate layers (Si_2O_5) attached to aluminum hydroxide layers ($Al_2(OH)_4$) are known as gibbsite layers. Silicate mineral layer with tetrahedral sheet and Al layer with octahedral sheet are interlinked. The surfaces of kaolin carry a constant structural negative charge derived from the isomorphous substitution of Si(IV) by Al(III) in silica layer [1, 5, 20-23]. In recent years, there is an increasing body of studies on dye adsorption from aqueous solutions onto kaolin supplied from different countries, such as basic yellow 28 [20], methylene blue [22-24], methyl orange [25] and congo red [4, 12].

Recently, the use of natural adsorbents such as kaolin to remove dyes from aqueous solution has increased. Although there are many studies on the adsorption of DR-28 using various adsorbents, the number of studies on DB-22 adsorption is very few. As mentioned earlier, DR-28 contains two azo group while DB-22 contains tetra-azo groups. In this research, the adsorption of diazo dye DR-28 and tetra-azo dye DB-22 onto calcined kaolin was compared. Kaolin obtained from Turkey was chosen as the adsorbent. Characteristics of the raw and calcined kaolin were discussed using SEM-EDS, FTIR, XRD, and TGA. The parameters such as calcination temperature of the adsorbent, adsorbent amount, initial pH of the dye solution, temperature, contact time and initial concentration of the dye solution were investigated. The adsorption isotherms (Langmuir, Freundlich and Temkin model), adsorption kinetics (pseudo first order, pseudo second order and intraparticle diffusion kinetic models), and thermodynamics properties were also examined.

EXPERIMENTAL

Materials

In this study, kaolin supplied from a company in Turkey was used to remove the diazo and tetra-azo dyes. HCl and NaOH were supplied from Tekkim. DR-28 and DB-22 were procured from Isolab (CAS No: 573-58-0, C.I. 22120) and HNY company respectively. The commercial name of DB-22 was Direct black-22 VSF 1600. Molecular structure of the dyes used in this study are given in Figure 1.

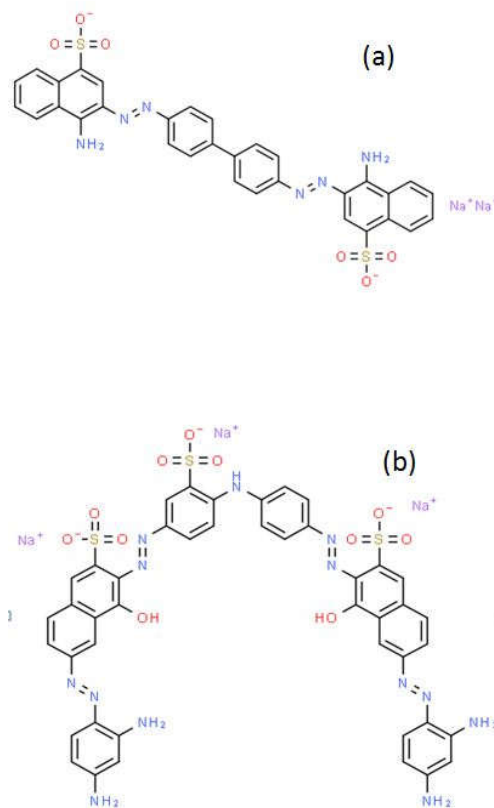


Figure 1. Chemical structure of (a) DR-28 and (b) DB-22.

Thermal treatment of kaolin

Kaolin was calcined using an oven (Proterm, PLF 120/5) at 200, 300, 400, and 500 °C for 3h. The uncalcined kaolin was coded as K. The calcined kaolin was coded with a reference to the calcination temperature, that is, K-200, K-300, K-400, and K-500.

Characterization of the kaolin

Characterization of the kaolin used in the study were performed by various techniques such as XRD (Rigaku Smart Lab), SEM-EDS (FEI, Quanta FEG250), TGA (SDT Q600) and FTIR (Perkin Elmer, Spectrum two).

Adsorption experiments

A stock solution was prepared by adding one gram of DR-28 or DB-22 dye to one liter of distilled water. Dye solutions at different concentrations were prepared using stock solution and distilled

water. The absorbance of the DR-28 and DB-22 solution were recorded using an UV-spectrophotometer (Hach, DR-2400) at a wavelength of 497nm and 481nm, respectively. After that, the standard curves were obtained for each dye.

For a typical run, a known amount of the adsorbent and 200 mL of dye solution was charged to the reaction vessel. The dye solution was magnetically stirred at a constant stirring speed of 500 rpm in all experiments. All the experiments were repeated two times. The following process variables were investigated: calcination temperature of kaolin (200-500 °C), contact time (10-120 min), pH (6-9), the initial dye concentration (20-50 mg/L), adsorbent amount (0.4-1.2 mg/200 mL) and temperature (20-50 °C). The samples taken from the dye solution centrifuged at 5000 rpm for 10 min. Then the absorbance of the sample was recorded to determine the dye concentration.

The removal of dye (R) was calculated using the Equation 1:

$$R, \% = [C_0 - C_t]/C_0 * 100 \quad (1)$$

The adsorption capacity of the adsorbent was calculated using the Equation 2:

$$q_e = [V * (C_0 - C_e)]/W \quad (2)$$

where q_e is the adsorption capacity of the adsorbent (mg/g). C_0 , C_t and C_e are the concentration of the dye (mg/L) at the beginning, at any time and at equilibrium, respectively. V (L) is the volume of the dye solution, and W (g) is the adsorbent weight.

Adsorption isotherms

In this study, the relationship between the dye molecules adsorbed on the calcined kaolin surface and the dye molecules remaining in the solution was investigated using widely used isotherm models such as Langmuir, Freundlich and Temkin. The Langmuir, Freundlich and Temkin models were estimated using the Eqs. (3), (4) and (5), respectively. The shape of the Langmuir isotherm (R_L) was calculated using the Eq. (6) [3, 20].

$$\frac{C_e}{q_e} = \frac{C_e}{q_{max}} + \frac{1}{q_{max}K_L} \quad (3)$$

$$\ln q_e = \ln k_f + \frac{1}{n} \ln C_e \quad (4)$$

$$q_e = \beta_1 \ln K_T + \beta_1 \ln C_e \quad (5)$$

$$R_L = 1/(1+K_L C_i) \quad (6)$$

where q_{max} (mg/g) is the adsorption capacity, K_L (L/g) is Langmuir constant related to the adsorption energy, R_L is the dimensionless separation factor in Langmuir isotherm. R_L value determines whether the adsorption process is irreversible ($R_L=0$), desirable ($0 < R_L < 1$), linear ($R_L=1$) or undesirable ($R_L > 1$) [1, 21]. K_f and n are the Freundlich constants. The value of n determines whether the adsorption process is physical ($n > 1$), chemical ($n < 1$) or linear ($n = 1$) [1]. K_T (L/mg) and β_1 (J/mol) are both known as Temkin isotherm constants [3].

Adsorption kinetics

Adsorption kinetics were determined using the experimental results. Pseudo first order (PFO), pseudo second order (PSO) and intra particle diffusion models were examined in the study. The Eq. 7 gives the linear form of the PFO kinetic model:

$$\ln(q_e - q_t) = \ln q_e - k_1 t \quad (7)$$

where q_e and q_t are the adsorption capacity at the equilibrium state (mg/g) and at any time (mg/g), respectively. Rate constant (k_1 , min^{-1}) is calculated from the slope of the graph plotted against $\ln (q_e - q_t)$ versus t [1].

Also, the PSO kinetic model is given in the Equation 8:

$$\frac{t}{q_t} = \frac{1}{k_2 q_e^2} + \frac{t}{q_e} \quad (8)$$

where k_2 (g/mg.min) is the rate constant of the PSO kinetics. Drawing the linear graph of t/q_t versus t can provide the PSO kinetic rate parameter [1, 20].

The intraparticle diffusion model is given in Equation 9:

$$q_t = K_i t^{0.5} + I \quad (9)$$

where K_i is the intra-particle diffusion rate constant (mg/g.min), and I is the width of the origin [26].

Thermodynamics behaviour

Eqs. (10), (11), and (12) were used to calculate the standard change of Gibbs free energy, enthalpy, and entropy in the adsorption process [27].

$$\Delta G^0 = -R T \ln K_D \quad (10)$$

$$\ln K_D = -\frac{\Delta G^0}{RT} = \frac{\Delta S^0}{R} - \frac{\Delta H^0}{RT} \quad (11)$$

$$K_D = \frac{C_A}{C_e} \quad (12)$$

where ΔG^0 (J/mol), ΔH^0 (J/mol), ΔS^0 (J/molK) are the standard change Gibbs free energy, the standard enthalpy change and the standard entropy change respectively. R is the universal gas constant (8.314J/molK), K_D is the equilibrium constant, C_A and C_e are the concentration of dye adsorbed and the concentration of dye remained after adsorption.

RESULTS AND DISCUSSION

Characterization

The SEM-EDS analysis was performed to examine the structure of the kaolin and to determine the elements it contains. SEM image and EDS spectra of the kaolin are given in Figure 2 (a-b). As shown in Fig 2a, the kaolin has porous and heterogeneous surface with various cavities. It has layered rectangular shapes. According to EDS analysis (Figure 2b), kaolin includes 19.66% carbon, 44.01% oxygen, 20.06% silicon, and 16.27% aluminum by weight. Figure 2 (c-d) shows the SEM image of K-200 and K-500. K-200 has layered irregular shapes with porous surface. K-500 has highly disordered structure. Layered structure of kaolin has been altered. It is seen that there was agglomeration of layers. Souri *et al.* [34] obtained similar result. Particle edges became more rounded and agglomeration of platelets in irregular stacks became more apparent.

XRD patterns of K and K-200 were analysed to investigate the influence of the calcination at 200 °C on the surface performance of kaolin. Figure 3a shows the XRD patterns. Kaolin has diffraction peaks at 12.34°, 24.87°, 26.61°, 50.1° and 59.93°. These peaks are related with kaolinite. In literature, Meroufel *et al.* [12] and Niu *et al.* [28] reported similar diffraction peaks. The diffraction peak at 20.86° and 62.3 are related with quartz [12].

When the kaolin and K-200 diffraction peaks were compared using Figure 3a, it was seen that the position of the peaks did not change. This shows that the crystal structure did not change. The intensity of the peaks at 2θ value of 12.34°, 24.87° and 26.61° decreased due to dehydroxylation [29-31].

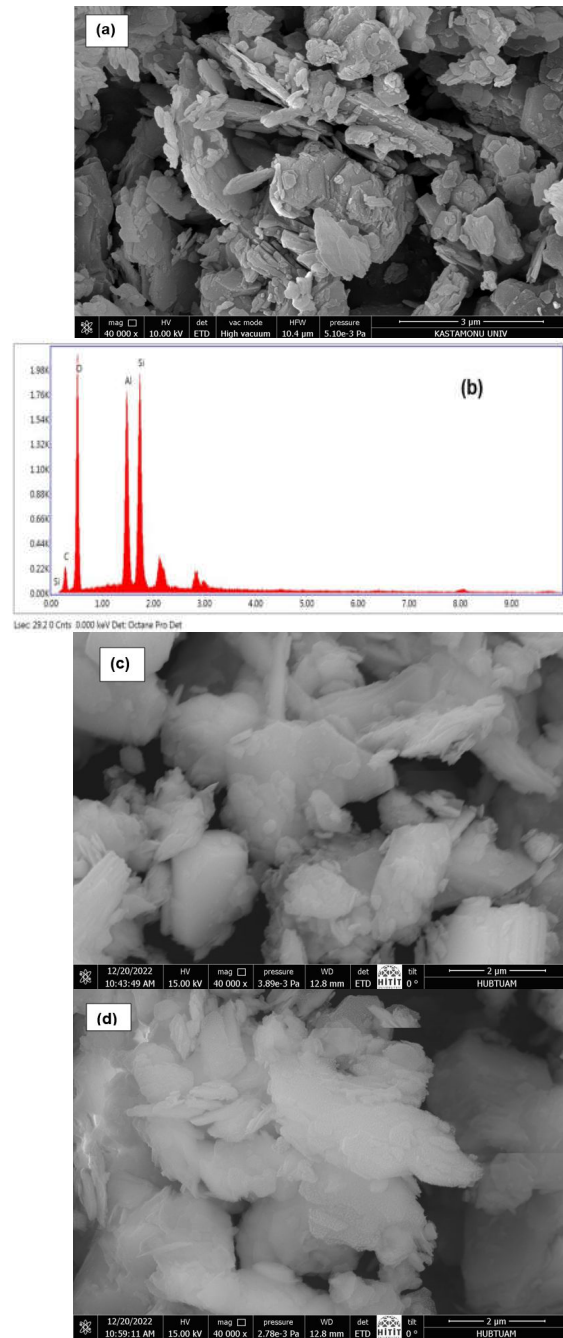


Figure 2. The SEM (a), EDS spectra (b) for kaolin, (c) SEM analysis of K-200, and (d) SEM analysis of K-500.

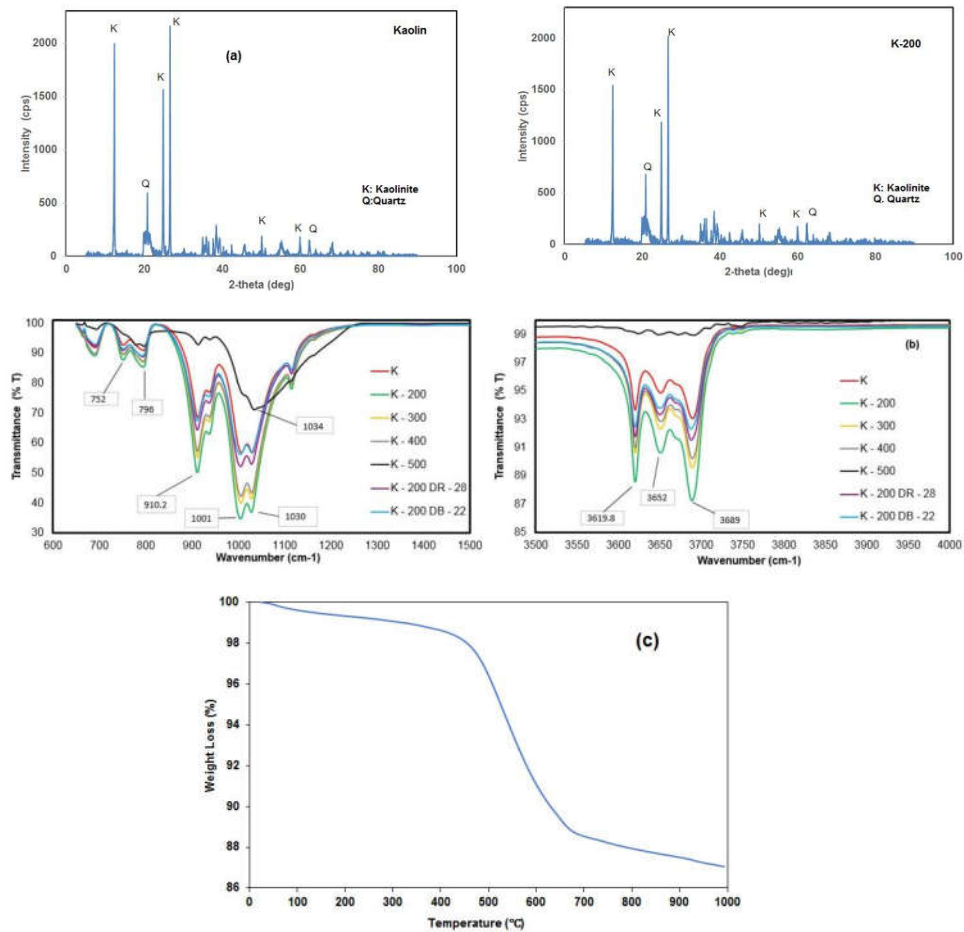


Figure 3. (a) XRD pattern of K and K-200, (b) FTIR analysis of adsorbents (K, K-200, K-300, K-400, K-500, K-200-DR-28, and K-200-DB-22), (c) TGA of kaolin.

FTIR analyses were performed to examine the functional groups of kaolin and calcined kaolin. The results are given in Figure 3b. The peaks around ~ 3690 and 3620 cm^{-1} were assigned to the stretching vibration of external and internal $-\text{OH}$ of kaolin [22, 23]. The band at $\sim 3690\text{ cm}^{-1}$ indicated the presence of hydroxyl groups (OH) in the interlayers of the kaolin sample, and the band at 3620 cm^{-1} was related to the O-H bonds pointing into the layers towards the tetrahedral sheets [32]. The band observed at 3690 cm^{-1} , indicated the amount of water physically adsorbed at the kaolin surface [3]. On the other hand, the absence of a characteristic band at 3670 cm^{-1} indicates that the kaolinite structure is disordered and easier to dehydrate [33]. The peaks at 1117, 1030, and 1001 cm^{-1} may be due to the tensile vibrations of the Si-O groups in the SiO_4 molecules (Si-O-Si stretching vibration related to presence of di-silicon oxide or quartz) [1, 12, 20, 22, 23,

28]. The peak at 910 cm^{-1} may be due to Al-OH-Al stretching vibration [22]. The peak at 796 cm^{-1} can be attributed to -OH deformation linked to Al [23, 24].

As shown in Figure 3b, IR functional bands of the raw kaolin and the calcined kaolin at 200, 300, and 400 °C were similar. The transmittance of the bands was observed to increase with the increase in calcination temperature. Gasparini *et al.* [29] reported similar results. The peak area of bands assigned in FTIR spectrum of kaolin increased with the decrease in calcination temperature. A similar result was reported by Tironi *et al.* [33]. As seen in Figure 3b, there was no band at 3670 cm^{-1} , and the structure of the kaolinite was disordered at lower temperatures due to dehydroxylation [34]. Below 500 °C, the absorbed water, free water, and hydrogen-bonded water in the kaolin can be released [35].

The peaks at ~ 3690 and 3620 cm^{-1} indicate the presence of kaolinite. These peaks were not observed in the kaolin calcined at 500 °C for 3 hours. This result showed that kaolin was transformed to metakaolin due to high temperature [32, 34, 35]. There were only several peaks at 1034 and 910 cm^{-1} at the calcination temperature of 500 °C.

The FTIR spectra of K-200 and the FTIR spectra of K-200 after DB-22 or DR-28 adsorption have the same bands. This indicates that the functional groups of K-200 were involved in the dye adsorption [23].

TGA analysis was performed to determine mass losses and thermal property of the kaolin. The high temperature treatment of kaolin converts it to metakaolin. The TGA of the kaolin is given in Figure 3c. Total mass loss was 12.27%. The adsorbed water in pores and on the surfaces of the kaolinite was removed below 400 °C [36]. A significant mass loss was observed between 400 and 650 °C due to thermal reaction of kaolinite and water molecules eliminated by dehydroxylation. Dehydroxylation of hydroxyl-containing compounds such as kaolinite occurs with the formation of water molecules as a result of the interaction of neighboring OH groups. OH groups released from octahedrally coordinated Al^{3+} ion provide a water formation. The metakaolinite was obtained after dehydroxylation [29, 36]. The TGA and FTIR results were consistent with each other.

Effect of calcination temperature of the kaolin

Calcined kaolin was tested, in order to determine the most effective adsorbent. The runs were carried out under the following reaction conditions: C_0 : 30 mg/L, T: 20 °C, adsorbent amount: 0.4 g/200 mL and initial pH: 7.3-7.4 (original). Figure 4 (a-b) shows the results. The removal rate decreased with the increase in the calcination temperature. The highest DR-28 removal was obtained with the K-200. DB-22 removal was almost the same with K and K-200 at 60min contact time. However, the DB-22 removal with K-200 was higher than K at 30 min contact time. As mentioned in previous section of the study, the transmittance of the bands increases up to 400 °C with an increasing calcination temperature. Kaolin phase structure changed and metakaolin was formed at the calcination temperature of 500 °C. At the calcination temperature of 200 °C, the lowest intensity was obtained and the functional groups involved dye molecules.

Effect of adsorbent amount

The effect of K-200 amount on the adsorption of dye was studied with the adsorbent amounts of 0.4, 0.6, 0.8, 1 and 1.2 g/200 mL while maintaining all the other parameters constant (C_0 : 30 mg/L, T: 20 °C, pH: original). As seen in Figure 4 (c-d), the removal of both dyes (DR-28 and DB-22) increased as the amount of K-200 increased. The reason for this is that as the amount of adsorbent increases, the adsorbent surface area and the number of active sites increase. 88.7% removal of DR-28 and 42.2% removal of DB-22 dyes were achieved with 1.2 g/200 mL under the studied conditions.

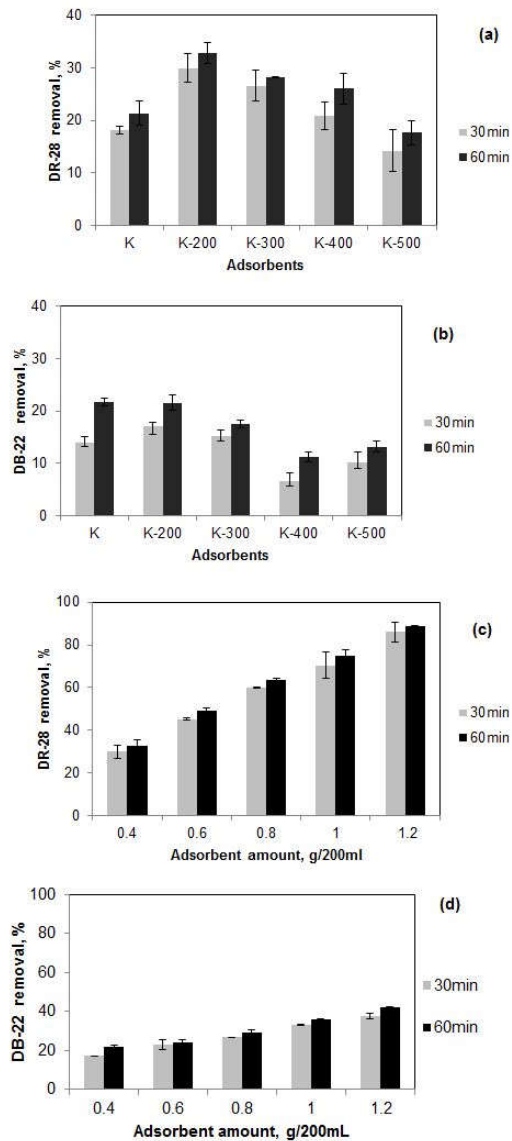


Figure 4. Effect of calcination temperature (a) DR-28 and (b) DB-22 (T: 20 °C, initial pH: original, C_0 : 30 mg/L, adsorbent amount: 0.4 g/200 mL) and effect of K-200 amount, (c) DR-28 and (d) DB-22 (adsorbent: K-200, T: 20 °C, initial pH: original, C_0 : 30 mg/L).

Aragaw and Angerasa [20] obtained similar results for the adsorption of Basic yellow on Ethiopian kaolin. In another study, the adsorption of Congo red on Australian kaolin was examined [37]. It was reported that the adsorption of Congo red increased with the increase of the adsorbent dosage, due to the increase in the adsorption surface area of micropores and the availability of adsorption sites. Mouni *et al.* [24] examined the removal of methylene blue using

kaolin and reported that the adsorption rate increased rapidly as the amount of adsorbent increased due to the increase in surface area and the availability of more adsorption sites.

In the present study, DB-22 removal was found to be lower than that of DR-28. As shown in Figure 1, the numbers of azo groups for DR-28 and DB-22 were different. DB-22 contains tetra-azo bonds while DR-28 contains two azo bonds. As the number of azo bonds increases, the stability of the dye increases and it becomes more difficult to remove the dye. On the other hand, the molecular weight of DB-22 (1084 g/mol) was higher than that of DR-28 (696.67 g/mol). As the number of azo bonds in azo dye increases, the molecular weight also increases. As the molecular weight of azo dyes increases, the dispersion of the dye in water increases. This causes a decrease in the azo dye removal rate [7].

Effect of the initial pH and temperature

One of the important parameters affecting the dye adsorption is the pH of the dye solution. Structure of DR-28 changes under strong acidic pHs due to the formation of protonated species (bluish color). The red color is stable within the pH range of 5-13 [12, 38]. Therefore, the pH range was determined as 6-9 in the study.

The effect of pH was studied using different initial pH settings (6, 8, 9 and original pH) while keeping the other parameters constant (T: 20 °C, C_0 : 30 mg/L, K-200 amount: 1.2 g/200 mL). The original pH of the dye solution was ≈ 7.4 . The experiment was started after the solution pH was adjusted and was not controlled during the experiment. The results are shown in Figure 5a.

The DR-28 removal rate increased from 80.7% to 88.9% with the increase of the solution pH from 6 to 7.4 (original pH). After this pH value, the removal of DR-28 decreased with the increase of the solution pH to 8, and then remained nearly constant. A similar behaviour was reported by Meorufel *et al.* [12] and Ogunmodede *et al.* [4]. The rate of Congo red removal using kaolin increased with the increase in pH, reached the maximum at pH 10, and then decreased at the higher pHs. The negatively charged adsorbent surface regions did not support the adsorption of the deprotonated Congo red due to electrostatic repulsion. Also, the abundance of OH^- ions in the basic solution creates a competitive environment for the adsorption sites with anionic Congo red ions causing reduced adsorption.

The removal of DB-22 decreased with the increase of pH from 6 to original pH. After this pH value, the removal rate remained nearly constant. A similar result was reported by Mahmodi *et al.* [39]. The adsorption capacity of DB-22 increased as the pH decreased. The electrostatic attraction between the positively charged adsorbent surface and the negatively charged dye is important at acidic pH values. As the pH of the system increases, the number of positively charged sites decreases.

Zeta potential analysis was used to determine surface charge of the K-200. As shown in Figure 5b, pH_{ZPC} value was 3.2 for adsorbent K-200. If the pH less than pH_{ZPC} value, adsorbent has positive charge, if pH greater than pH_{ZPC} adsorbent has negative charge [26]. Below pH_{ZPC} value, electrostatic attraction exists between negative charges of anionic dyes and positive charges of K-200 [3, 37]. At pH above pH_{ZPC} value, ionic repulsion between the K-200 surface and anionic dye molecules occur [37].

The effect of solution temperature on the adsorption of DR-28 and DB-22 dyes on the K-200 adsorbent was investigated at 20, 30, 40, and 50 °C while keeping other parameters constant (C_0 : 30 mg/L, K-200 amount: 1.2 g/200 mL, initial pH: original).

As shown in Figure 5c, the removal of DR-28 in 60 min decreased from 88.7% to 86%, 81.1%, and 64% with the increase in temperature from 20 to 30, 40, and 50 °C, respectively. The decrease in the removal rate with the increasing adsorption temperatures shows that the adsorption process occurred under exothermic conditions. The dye molecules on the adsorbent surface may have an increased tendency to move away with the increasing temperatures so, the removal rate of dye decreases [1]. In their study, Aragaw *et al.* [20] reported that the adsorbent pores expanding with the increasing temperatures caused the dye molecules not to be kept in an active site.

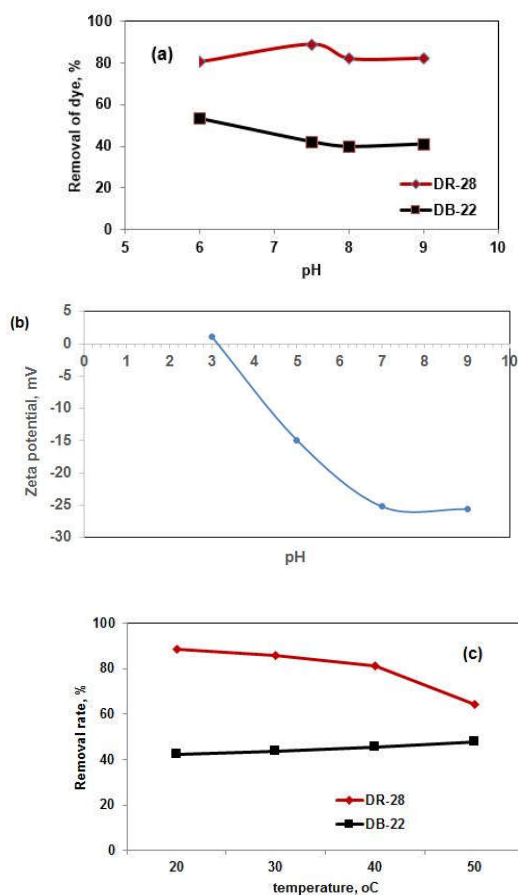


Figure 5. (a) Effect of initial pH (T: 20 °C, C_0 : 30 mg/L, K-200 amount: 1.2 g/200 mL, contact time: 60 min), (b) Zeta potential of K-200, and (c) effect of temperature (initial pH: original, K-200 amount: 1.2 g/200 mL, C_0 : 30 mg/L, contact time: 60 min).

The removal rate of DB-22 in 60 min was 42.2%, 43.6%, 45.6% and 48% at 20, 30, 40, and to 50°C, respectively. The increase in the removal rate with the increasing temperatures shows that the adsorption process was endothermic. As a result of the increased mobility of dye molecules at high temperatures, the possibility of an interaction between dye molecules and active sites on the adsorbent surface increases [22, 24]. As the solution temperature increases, the solution viscosity decreases and the transport of dye molecules to the adsorbent surface by external diffusion and diffusion inside the pores becomes easier [3, 24].

Effect of initial dye concentration and contact time

The effects of contact time and initial concentration of DR-28 and DB-22 dyes using K-200 were studied with initial dye concentrations (20-50 mg/L) and contact time (0-120 min) while the other parameters were kept constant (K-200 amount: 1.2 g/200 mL, T: 20 °C, initial pH: original). The results are shown in Figure 6.

The removal of DB-22 and DR-28 increased very quickly as the contact time increased to 20 min, and then it slightly increased until a contact time of 45 min, and reached the equilibrium state. No further increase was observed in the removal of both dyes with the increasing contact times. In the initial stage, many active sites of the K-200 were available. Therefore, the removal rate increased until reaching the equilibrium within 45 min. After a contact time of 45 min, the number of empty sites on K-200 decreased, and thus, the removal rate also decreased.

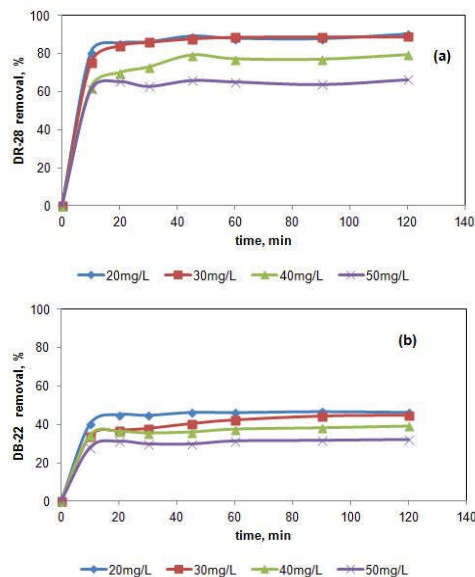


Figure 6. Effect of initial dye concentration and contact time (a) DR-28 and (b) DB-22 (T: 20 °C, initial pH: original, K-200 amount: 1.2 g/mL).

As seen in Figure 6, the removal of dye decreased with the increase in the initial concentration. The removal rate of DR-28 in a contact time of 120 min decreased from 90.1% to 88.9%, 79.4% and 66.3% with the increase in the initial dye concentration from 20 to 30, 40, and 50 mg/L, respectively. A similar result was obtained for the removal of DB-22. The removal rate of DB-22 decreased from 46.2% to 44.6%, 39.3% and 32.3% with the increase in the initial dye concentrations from 20 to 30, 40, and 50 mg/L, respectively. The ratio of the active surface area of the adsorbent to the dyes in the solution is important. According to the results, this ratio was high at the low concentrations of DR-28 and DB-22. At high concentrations, there are less active sites on the adsorbent than the dye molecules in the solution. As a result, the initial concentration of 20 mg/L was the optimum initial concentration. At low dye concentrations, active sites on the adsorbent surface are enough for the adsorption, and as a result the removal efficiency of dye is high. At high dye concentrations, the removal rate decreases due to the fact that the active sites of the adsorbent are occupied and the dye molecules re-enter the liquid phase [20].

In the literature, there are some studies reported similar results. In a previous study, it was reported that the removal of Basic yellow 28 on the Ethiopian kaolin decreased with the increase of initial concentration from 20 to 60 mg/L [20]. In another study, it was reported that Congo red removal on the Algerian kaolin reached the equilibrium after 40 min and adsorption capacity of the kaolin increased with the increase in the initial concentration [12]. In their study, Vimonses *et al.* [37] reported that the dye removal decreased with the increase of the initial dye concentration from 50 to 250 mg/L due to the limitation of adsorption sites on the clay mineral surface.

Adsorption isotherms

The adsorption isotherm models (Langmuir, Freundlich and Temkin) were calculated with different initial dye concentrations (20-50 mg/L). The other parameters were kept constant (initial pH: original, K-200 amount: 1.2 g/200 mL, T: 20 °C). Table 1 gives the Langmuir, Freundlich and Temkin isotherm parameters for DR-28 and DB-22 adsorption. Figure 7a shows the Langmuir adsorption isotherm models for DR-28 and DB-22 on K-200.

In the Langmuir model, R^2 was 0.9964 for DR-28, and 0.9542 for DB-22. In the Freundlich model, R^2 was 0.6805 for DR-28, and 0.7928 for DB-22. In the Temkin model R^2 was 0.714 for DR-28, and 0.812 for DB-22. The Langmuir isotherm has high regression coefficient than other isotherms. It can be said that the adsorption of both dyes were compatible with the Langmuir isotherm. Based on the calculated R_L values for DB-22 and DR-28, the adsorption process was defined as desirable. According to Langmuir isotherm model, adsorbent can be adsorbed as a monolayer from the homogeneous adsorbent materials. Adsorbent surface is uniform, and adsorption capacity is the same at all points [28].

The maximum adsorption capacity of K-200 was determined as 5.39 and 3.5 mg/g for DR-28 and DB-22 respectively. In the literature, there are studies on the adsorption of dye with kaolin obtained from different countries. In one study, adsorption of Basic yellow investigated using Ethiopian kaolin and adsorption capacity was found to be 0.885 mg/g [20]. Merufel *et al.* [12] and Vimonses *et al.* [37] used Algerian and Australian kaolin for the adsorption of Congo red, adsorption capacity found as 5.94 mg/g and 5.44 mg/g, respectively. In another study, Dias *et al.* [40] investigated adsorption of annatto dye on Brazil kaolin. Adsorption capacity was 12.9 mg/g at 60 °C. As a result, the K-200 has nearly similar performance in removing of DR-28 and DB-22 from aqueous solution compared to kaolin obtained from other countries.

Table 1. The parameters of the adsorption isotherms for DB-22 and DR-28 dye adsorption.

Model	Constants	DR-28	DB-22
Langmuir	q_{max} (mg/g)	5.39	3.50
	K_L (L/mg)	0.935	0.103
	R^2	0.9964	0.9542
	R_L	0.021-0.054	0.163-0.327
Freundlich	n	5.18	2.69
	K_f (mg/g)	3.18	0.76
	R^2	0.6805	0.7928
Temkin	β_1 (J/mol)	0.91	0.979
	K_T (L/mg)	12.54	2.05
	R^2	0.714	0.812

Adsorption kinetics

Kinetic behaviour of DR-28 and DB-22 adsorption using K-200 was studied in 10-120 min contact time. The pseudo first order (PFO), pseudo second order (PSO) and intraparticle diffusion kinetics models were used. Table 2 gives the parameters of the PFO, PSO and intraparticle diffusion models for DR-28 and DB-22 adsorption onto K-200. Figure 7b and 7c shows the results of the PSO and intraparticle diffusion kinetic model of DR-28 and DB-22 with K-200. As shown in Table 2, the correlation coefficient (R^2) of the PSO was higher than that of the PFO. The calculated q values in the PSO model and the experimental q values are close to each other. According to the results, the model that best describes the DR-28 and DB-22 adsorption kinetics was PSO.

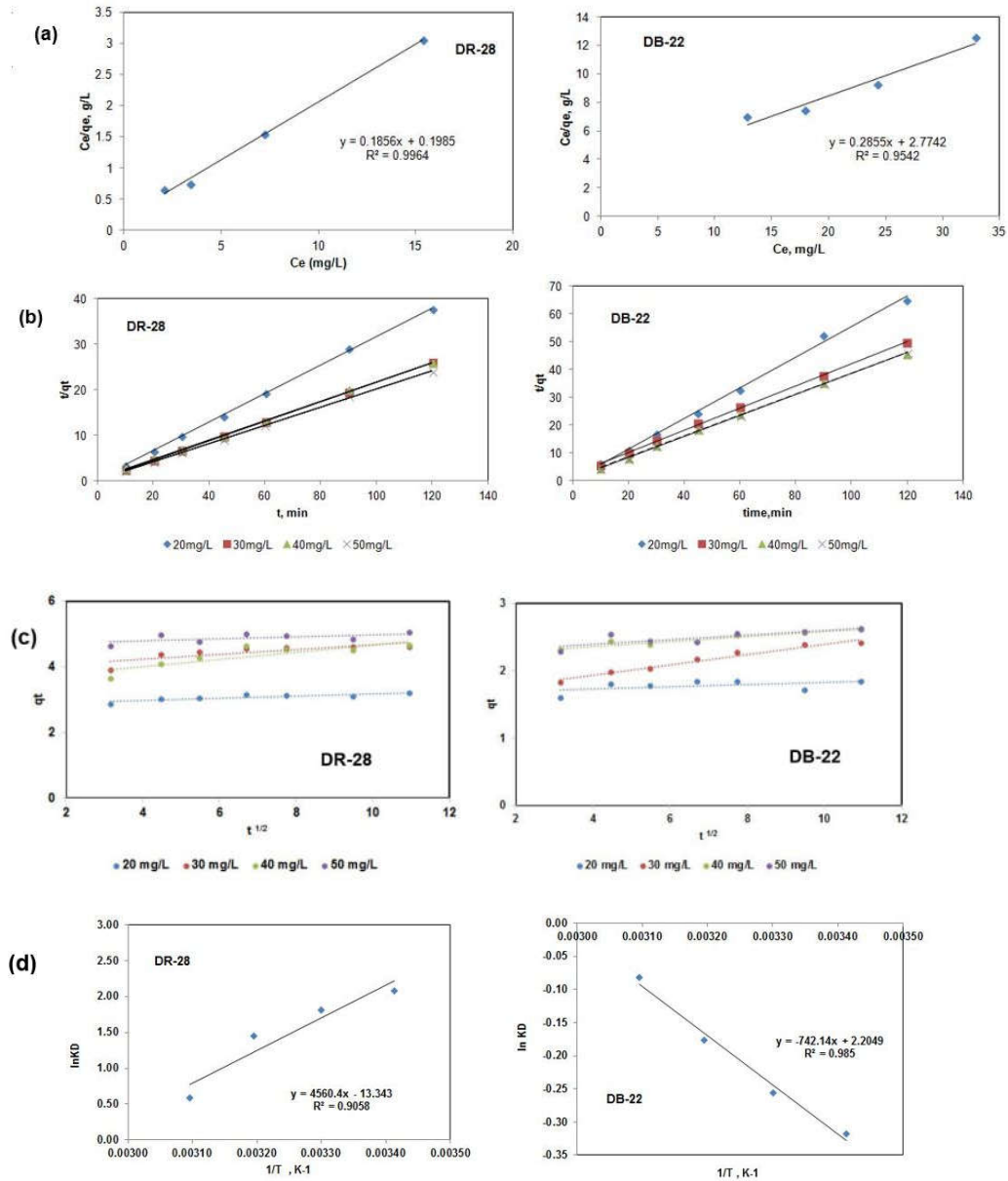


Figure 7. (a) Langmuir isotherm (T: 20 °C, initial pH: original, K-200 amount: 1.2 g/mL, contact time: 120 min), (b) PSO kinetic model (T: 20 °C, initial pH: original, K-200 amount: 1.2 g/mL, contact time: 120 min), (c) intra particle diffusion model, (d) thermodynamics of DR-28 and DB-22 adsorption on K-200 (initial pH: original, K-200 amount: 1.2 g/200 mL, C_0 : 30 mg/L, contact time: 60 min).

The intra-particle diffusion model is widely used in the study of the kinetic behavior of the adsorption of pollutants and can reasonably interpret the mechanism of the adsorption process [26]. According to this model, if the q_t plot vs. $t^{0.5}$ is a straight line, the intra-particle diffusion is the limiting step in the adsorption process and if it is not a straight line, the adsorption process follows the liquid film diffusion [1, 27]. As shown in Figure 7c, the plot of q^t against $t^{0.5}$ was linear, it can be said that the adsorption of DR-28 and DB-22 was controlled by intraparticle diffusion mechanism.

Table 2. PFO, PSO and intraparticle diffusion kinetic models constants for DR-28 and DB-22 adsorption using the adsorbent K-200.

Dye	Kinetic	Parameters	C_0 (mg/L)			
			20	30	40	50
DR-28	PFO	R^2	0.395	0.9909	0.218	0.32
		k_1	0.016	0.069	0.027	0.0056
		q_{cal}	0.225	1.159	1.787	0.164
		q_{exp}	3.19	4.6	4.64	5.03
	PSO	R^2	0.9996	0.9999	0.9992	0.9990
		k_2	0.234	0.142	0.076	0.24
		q_{cal}	3.2	4.67	4.72	5.01
		q_{exp}	3.19	4.6	4.64	5.03
	Intraparticle diffusion	K_i	0.0341	0.0740	0.1108	0.0312
		I	2.832	3.925	3.568	4.668
		R^2	0.709	0.649	0.708	0.364
DB-22	PFO	R^2	0.062	0.9621	0.8839	0.6036
		k_1	0.011	0.0383	0.0192	0.0233
		q_{cal}	0.045	0.5573	0.195	0.150
		q_{exp}	0.981	1.281	1.399	1.395
	PSO	R^2	0.9968	0.9991	0.9992	0.9993
		k_2	1.650	0.131	0.256	0.327
		q_{cal}	0.977	1.338	1.417	1.412
		q_{exp}	0.981	1.281	1.399	1.395
	Intraparticle diffusion	K_i	0.162	0.0776	0.0372	0.0337
		I	1.662	1.618	2.212	2.261
		R^2	0.261	0.963	0.898	0.641

Thermodynamic study

To understand the behaviour of the adsorption process, thermodynamic parameters (ΔG^0 , ΔH^0 , ΔS^0) were calculated using the Equations (10), (11), and (12). The adsorption of DR-28 and DB-22 dyes on the K-200 adsorbent were thermodynamically studied in the temperature range of 20-50 °C while the other parameters constant (C_0 : 30 mg/L, K-200 amount: 1.2 g/200 mL, a contact time: 60 min, pH: original). Figure 7d gives the results of the thermodynamic study. The calculated thermodynamic parameters (ΔG^0 , ΔH^0 , ΔS^0) are given in Table 3.

The value of enthalpy changes (ΔH^0) for DR-28 dyes was found to be negative, which means that, the removal of DR-28 was exothermic. A negative ΔS^0 value for the adsorption of DR-28 indicates that, there is a decrease in the energy available at the solid/solution interface and there is no significant change in the internal structure of the adsorbent after the adsorption [40]. According to Boushehrian *et al.* [1], negative ΔS^0 value in dye adsorption indicates a decrease in random collision of dye molecules and adsorbent surface in the adsorption process. In the present study, ΔG^0 was found to be negative at the studied temperatures. The negative values of ΔG^0 indicate that the adsorption process is feasible and spontaneous [37, 38, 41].

Table 3. Thermodynamic parameters for DB-22 and DR-28.

Dye	T (°C)	ΔH^0 (kJ/mol)	ΔS^0 (J/molK)	ΔG^0 (kJ/mol)
DR-28	20	-37.92	-110.93	-5.071
	30			-4.575
	40			-3.786
	50			-1.562
DB-22	20	6.17	18.33	0.773
	30			0.644
	40			0.459
	50			0.219

On the other hand, a positive value of ΔH^0 for DB-22 dye showed that the adsorption process was endothermic. A positive value of ΔS^0 suggests that there is an increase in randomness at the dye and adsorbent interface during the adsorption process [2]. The value of ΔG^0 decreased from 0.773 to 0.219 kJ/mol with the increase of temperature. The positive values of ΔG^0 indicate that adsorption is non spontaneous. According to results, adsorption process was a combination of physical and chemical adsorption within a temperature range of 20-50 °C [22].

CONCLUSIONS

In this research, the adsorption of DR-28 and DB-22 was investigated using a calcined kaolin. Kaolin was calcined at different temperatures. The characteristics of the adsorbent were determined by SEM-EDS, FTIR, XRD, and TGA analyzes. The kaolin calcined at 200 °C was found to be the most effective adsorbent in removing dyes used in the study. The results showed that the removal of the tetra-azo dye DB-22 was more difficult than that of the diazo dye DR-28. The removal rates of DR-28 and DB-22 were 90.1% and 46.2%, respectively at the initial concentration of 20mg/L, original pH, 20 °C and in the adsorbent amount of 1.2 g/200 mL. In the study, the adsorption isotherms, kinetics, and thermodynamic behaviors of the adsorption process of DR-28 and DB-22 dyes were investigated using calcined kaolin at 200 °C. The experimental results were better fitted to the Langmuir isotherm model. Based on this result, it was understood that the adsorption process took place on the homogeneous surface. The kinetic behavior of the adsorption process showed that the pseudo second order model provided a better fit to the experimental data. The adsorption of DB-22 was endothermic while that of DR-28 was exothermic.

REFERENCES

1. Boushehrian, M.M.; Hossein, E.H.; Foroutan, R. Ultrasonic assisted synthesis of Kaolin/CuFe₂O₄ nanocomposite for removing cationic dyes from aqueous media. *J. Environ. Chem. Eng.* **2020**, *8*, 103869.
2. Fardjaoui, N.; El Berrichi, F.Z.; Ayari, F. Kaolin-issued zeolite A as efficient adsorbent for Bezanyl Yellow and Nylomine Green anionic dyes. *Micropor. Mesopor. Mater.* **2017**, *243*, 91-101.
3. Magdy, A.; Fouad, Y.O.; Abdel-Aziza, M.H.; Konsowa, A.H. Synthesis and characterization of Fe₃O₄/kaolin magnetic nanocomposite and its application in wastewater treatment. *J. Ind. Eng. Chem.* **2017**, *56*, 299-311.
4. Ogunmodede, O.T.; Ojo, A.A.; Adewole, E.; Adebayo, O.L. Adsorptive removal of anionic dye from aqueous solutions by mixture of Kaolin and Bentonite clay: Characteristics, isotherm, kinetic and thermodynamic studies. *Iran. J. Energy. Environ.* **2015**, *6*, 147-153.
5. Kausar, A.; Iqbal, M.; Javeda, A.; Aftab, K.; Nazli, Z.; Bhatti, H.N.; Nouren, S. Dyes adsorption using clay and modified clay: A review. *J. Mol. Liq.* **2018**, *256*, 395-407.

6. Benkhaya, S.; M'rabet, S.; El Harfi, A. A review on classifications, recent synthesis and applications of textile dyes. *Inorg. Chem. Commun.* **2020**, 115, 107891.
7. Foroutan, R.; Peighambaroust, S.J.; Hemmati, S.; Khatooni, H.; Ramavandi, B.; Preparation of clinoptilolite/starch/CoFe₂O₄ magnetic nanocomposite powder and its elimination properties for cationic dyes from water and wastewater. *Int. J. Biol. Macromol.* **2021**, 189, 432-442.
8. Benkhaya, S.; M'rabet, S.; El Harfi, A. Classifications, properties, recent synthesis and applications of azo dyes. *Heliyon* **2020**, 6, e03271.
9. Adebayo, M.A.; Adebomi, J.I.; Abe, T.O.; Areo, F.I. Removal of aqueous Congo red and malachite green using ackee apple seed-bentonite composite. *Colloids. Interf. Sci. Commun.* **2020**, 38, 100311.
10. Guy, N.; Ozacar, M. The influence of noble metals on photocatalytic activity of ZnO for Congo red degradation. *Int. J. Hydrog. Energy* **2016**, 41, 20100-20112.
11. Kataria, N.; Garg, V.K.; Removal of Congo red and Brilliant green dyes from aqueous solution using flower shaped ZnO nanoparticles. *J. Environ. Chem. Eng.* **2017**, 5, 5420-5428.
12. Meroufel, B.; Benali, O.; Benyahia, M.; Benmoussa, Y.; Zenasni, M.A. Adsorptive removal of anionic dye from aqueous solutions by Algerian kaolin: Characteristics, isotherm, kinetic and thermodynamic studies. *J. Mater. Environ. Sci.* **2013**, 4, 482-491.
13. Hien, N.T.; Nguyen, L.H.; Van, H.T.; Nguyen, T.D.; Nguyen, T.H.V.; Chu, T.H.H.; Nguyen, T.V.; Trinh, V.T.; Vu, X.H.; Aziz, K.H.H. Heterogeneous catalyst ozonation of Direct Black 22 from aqueous solution in the presence of metal slags originating from industrial solid wastes. *Sep. Purif. Technol.* **2020**, 233, 115961.
14. Moradzadeh, A.; Mahjoub, A.; Sadjadi, M.S.; Sadr, M.H.; Farhadyar, N. Investigation on synthesis, characterization and photo catalytic degradation of Congo red by Zn-doped CdTiO₃/TiO₂. *Polyhedron* **2019**, 170, 404-411.
15. Tanwar, R.; Kumar, S.; Mandal, U.K. Photocatalytic activity of PANI/Fe⁰ doped BiOCl under visible light-degradation of Congo red dye. *J. Photochem. Photobiol. A: Chem.* **2017**, 333, 105-116.
16. Patel, H.; Vashi, R.T. Removal of Congo Red dye from its aqueous solution using natural coagulants. *J. Saudi Chem. Soc.* **2012**, 16, 131-136.
17. Gomes, R.K.M.; Santana, R.M.R.; Moraes, N.F.S.; Júnior, S.G.S.; Lucena, A.A.; Zaidan, L.E.; Elihimas, D.R.M.; Napoleao, D.C. Treatment of direct black 22 azo dye in led reactor using ferrous sulfate and iron waste for Fenton process: Reaction kinetics, toxicity and degradation prediction by artificial neural Networks. *Chem. Pap.* **2021**, 75, 1993-2005.
18. Khadhraoui, M.; Trabelsi, H.; Ksibi, M.; Bouguerra, S.; Elleuch, B. Discoloration and detoxification of a Congo red dye solution by means of ozone treatment for a possible water reuse. *J. Hazard. Mater.* **2009**, 161, 974-981.
19. Das, R.; Bhaumik, M.; Giri, S.; Maity, A. Sonocatalytic rapid degradation of Congo red dye from aqueous solution using magnetic Fe⁰/polyaniline nanofibers. *Ultrason. Sonochem.* **2017**, 37, 600-613.
20. Aragaw, T.A.; Angerasa, F.T. Synthesis and characterization of Ethiopian kaolin for the removal of basic yellow (BY 28) dye from aqueous solution as a potential adsorbent. *Heliyon* **2020**, 6, e04975.
21. Chen, Z.; Cheng, Y.; Chen, Z.; Megharaj, M.; Naidu, R. Kaolin-supported nanoscale zero-valent iron for removing cationic dye-crystal violet in aqueous solution. *J. Nanopart. Res.* **2012**, 14, 899.
22. Huang, Q.; Liu, M.; Chen, J.; Wang, K.; Xu, D.; Deng, F.; Huang, H.; Zhang, X.; Wei, Y. Enhanced removal capability of kaolin toward methylene blue by mussel-inspired functionalization. *J. Mater. Sci.* **2016**, 51, 8116-8130.

23. Jawad, A.H.; Abdulhameed, A.S. Mesoporous Iraqi red kaolin clay as an efficient adsorbent for methylene blue dye: Adsorption kinetic, isotherm and mechanism study. *Surf. Interface* **2020**, *18*, 100422.
24. Mouni, L.; Belkhiri, L.; Bollinger, J.; Bouzaza, A.; Assadi, A.; Tirrib, A.; Dahmoune, F.; Madani, K.; Remini, H. Removal of Methylene Blue from aqueous solutions by adsorption on Kaolin: Kinetic and equilibrium studies. *Appl. Clay Sci.* **2018**, *153*, 38-45.
25. Liu, D.; Dong, C.; Zhong, J.; Rena, S.; Chena, Y.; Qiu, T. Facile preparation of chitosan modified magnetic kaolin by one-pot coprecipitation method for efficient removal of methyl orange. *Carbohydr. Polym.* **2020**, *245*, 116572.
26. Hosseini, S.S.; Hamadi, A.; Foroutan, R.; Peighambaroust, S.J.; Ramavandi, B. Decontamination of Cd²⁺ and Pb²⁺ from aqueous solution using a magnetic nanocomposite of eggshell/starch/Fe₃O₄. *J. Water Proc. Eng.* **2022**, *48*, 102911.
27. Safarzadeh, H.; Peighambaroust, S.J.; Mousavi, S.H.; Foroutan, R.; Mohammadi, R.; Peighambaroust, S.H. Adsorption ability evaluation of the poly(methacrylic acid-co-acrylamide)/cloisite 30B nanocomposite hydrogel as a new adsorbent for cationic dye removal. *Environ. Res.* **2022**, *212*, 113349.
28. Niu, S.; Xie, X.; Wang, Z.; Zheng, L.; Gao, F.; Miao, Y. Enhanced removal performance for Congo red by coal-series kaolin with acid treatment. *Environ. Technol.* **2021**, *42*, 1472-1481.
29. Gasparini, E.; Tarantino, S.C.; Ghigna, P.; Riccardi, M.P.; Cedillo-González, E.I.; Siligardi, C.; Zema, M. Thermal dehydroxylation of kaolinite under isothermal conditions. *Appl. Clay Sci.* **2013**, *80-81*, 417-425.
30. Peng, H.; Vaughan, J.; Vogrin, J. The effect of thermal activation of kaolinite on its dissolution and reprecipitation as zeolites in alkaline aluminate solution. *Appl. Clay Sci.* **2018**, *157*, 189-197.
31. Yan, K.; Guo, Y.; Fang, L.; Cui, L.; Cheng, F.; Li, T. Decomposition and phase transformation mechanism of kaolinite calcined with sodium carbonate. *Appl. Clay Sci.* **2017**, *147*, 90-96.
32. Khan, M.I.; Khan, H.U.; Azizli, K.; Sufiana, S.; Mana, Z.; Siyal, A.A.; Muhammad, N.; Rehman, M. The pyrolysis kinetics of the conversion of Malaysian kaolin to metakaolin. *Appl. Clay Sci.* **2017**, *146*, 152-161.
33. Tironi, A.; Trezza, M.A.; Irassar, E.F.; Scian, A.N. Thermal treatment of kaolin: effect on the pozzolanic activity. *Proc. Mater. Sci.* **2012**, *1*, 343-350.
34. Souri, A.; Golestani-Fard, F.; Naghizadeh, R.; Veisheh, S. An investigation on pozzolanic activity of Iranian kaolins obtained by thermal treatment. *Appl. Clay Sci.* **2015**, *103*, 34-39.
35. Feng, H.; Li, C.; Shan, H. Effect of calcination temperature of kaolin microspheres on the in situ synthesis of ZSM-5. *Catal. Lett.* **2009**, *129*, 71-78.
36. Cheng, H.; Liu, Q.; Yang, J.; Mac, S.; Frost, R.L. The thermal behavior of kaolinite intercalation complexes-A review. *Thermochim. Acta* **2012**, *545*, 1-13.
37. Vimonse, V.; Lei, S.; Jin, B.; Chow, C.W.K.; Saint, C. Adsorption of Congo red by three Australian kaolins. *Appl. Clay Sci.* **2009**, *43*, 465-472.
38. Olusegun, S.J.; Mohallem, N.D.S. Comparative adsorption mechanism of doxycycline and Congo red using synthesized kaolinite supported CoFe₂O₄ nanoparticles. *Environ. Pollut.* **2020**, *260*, 114019.
39. Mahmoodi, N.M.; Najafi, F.; Khorramfar, S.; Amini, F.; Arami, M. Synthesis, characterization and dye removal ability of high capacity polymeric adsorbent: Polyaminoimide homopolymer. *J. Hazard. Mater.* **2011**, *198*, 87-94.
40. Dias, M.; Valério, A.; Oliveiro, D.; Ulson de Souza, A.A.; Ulson de Souza, S.M. Adsorption of natural annatto dye by kaolin: kinetic and equilibrium. *Environ. Technol.* **2020**, *41*, 2648-2656.
41. Shirsath, S.R.; Patil, A.P.; Bhanvase, B.A.; Sonawane, B.A.; Ultrasonically prepared poly(acrylamide)-kaolin composite hydrogel for removal of crystal violet dye from wastewater. *J. Environ. Chem. Eng.* **2015**, *3*, 1152-1162.